Supporting Information

SI Materials and Methods

General methods for chemical synthesis
All solvents and reagents were obtained from commercial sources and were used without further purification. NMR spectra were recorded on a Varian 400 MHz 400-MR spectrometer. NMR chemical shifts are expressed in ppm relative to internal solvent peaks, and coupling constants are measured in Hz. High resolution mass spectra were recorded at the Small Molecule Mass Spectrometry Facility at Harvard University by electrospray ionization (ESI) on an Agilent 6550 q-TOF instrument.

Synthesis of 15-azi-palmitic acid

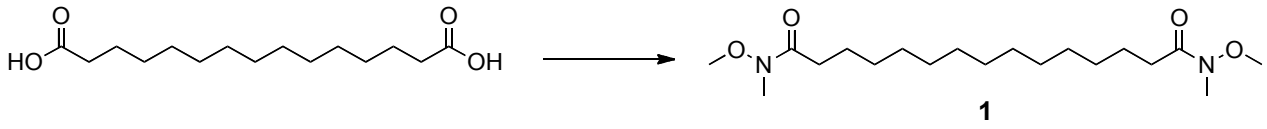

1

1,15-(N-methoxy-N-methyl)-pentadecanediacetamide (1). 1,15-pentadecanedicarboxylic acid (13g, 47.7mmol) was dissolved in dry dichloromethane (100 mL) and triethylamine (13.3mL, 95.4mmol, 2 equivalents). Carbonyldiimidazole (17g, 105mmol, 2.2equivalents) dissolved in dry dichloromethane (50 mL) was then added in one portion, and the reaction was incubated at room temperature, with vigorous stirring under dry Argon atmosphere. After 2 hours, during which a white precipitate appeared, N,O-dimethylhydroxylamine hydrochloride (10g, 105mmol, 2.2equivalents) was added in one portion to the reaction. The white precipitate dissolved within 10 minutes and the reaction was incubated for an additional 2 hours at room temperature. The reaction was quenched with 1M HCl, and the aqueous phase was extracted 3 times with dichloromethane. The combined organic layers were washed with 1M HCl in brine, dried on sodium sulfate, and the solvent was evaporated under reduced pressure, yielding essentially pure compound **1** (16 grams, 94%).

^{1}H NMR (400MHz, $CDCl_3$) δ 3.64 (s, 6 H), 3.14 (s, 6 H), 2.37 (t, J = 7.5 Hz, 4 H) 1.58 (quint, J = 7.2, 4 H), 1.21 (comp, 18 H); ^{13}C NMR (100MHz, $CDCl_3$) δ 176.96, 61.24, 29.67, 29.65, 29.54, 29.49, 29.47, 24.72.

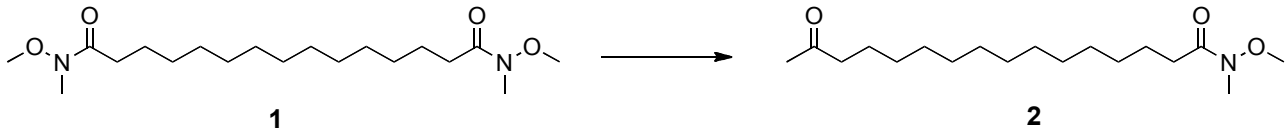

1 **2**

15-keto-1-(N-methoxy-N-methyl)-hexadecanamide (2). Compound **1** (16g, 45mmol) was dissolved in dry THF (450mL) in a flame-dried, 1L round-bottom flask, under dry Argon. The solution was cooled on ice, and methylmagnesium bromide (12mL of a 3M solution in THF, 36mmol, 0.8equivalents) was added over 2 hours, with stirring. The reaction was quenched with 1M HCl, extracted with ethyl acetate, and the organic layer was washed with saturated sodium bicarbonate and brine. The solvent was evaporated under reduced pressure, the residue was dissolved in 25% ethyl acetate/hexanes, and was passed through a thick pad of silica gel (300g). Product **2** and the double-addition product (2,16-heptadecanedione) were eluted with 500mL 40% ethyl acetate/hexanes, followed by elution of unreacted starting material with 500mL dichloromethane. The reaction was repeated two more times on the recovered starting material, and the products were pooled to give 10g of product **2** mixed with 2,16-heptadecanedione (69% combined yield). The mixed products were used in the next step without further purification. For analytical purposes, we obtained pure compound **2** by fractionating a small portion of the mixed products by flash chromatography (25-75% linear gradient ethyl acetate/hexanes). Under these conditions, contaminating 2,16-heptadecanedione elutes at 5-10% ethyl acetate/hexanes, while compound **2** elutes at 40-50% ethyl acetate/hexanes.

^{1}H NMR (400MHz, $CDCl_3$) δ 3.67 (s, 3 H), 3.17 (s, 3 H), 2.40 (t, *J* = 7.4, 4 H), 2.12 (s, 3H), 1.61 (quint, *J* = 7.6, 2H), 1.55 (quint, *J* = 7.0, 2 H), 1.24 (comp, 18 H); ^{13}C NMR (100MHz, $CDCl_3$) δ 209.54, 174.95, 61.31, 43.96, 32.06, 29.98, 29.73, 29.71, 29.62, 29.60, 29.55, 29.52, 29.31, 24.79, 24.00. HRMS (ESI-q-TOF) m/z: $[M+H]^+$ Calculated for $C_{18}H_{36}NO_3$ 313.2690; Found 313.2708, $[M+Na]^+$ Calculated for $C_{18}H_{35}NO_3Na$ 336.2509; Found 336.2525.

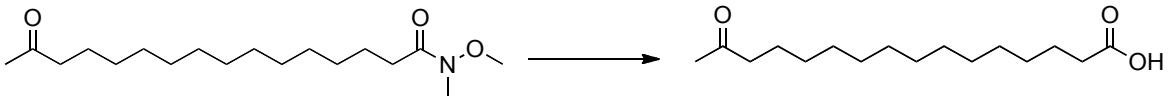

2 **3**

15-oxo-hexadecanoic acid (3). A mixture of compound **2** and 2,16-heptadecanedione (10g) was dissolved in methanol (25mL), and potassium hydroxide was added (6.25mL of a 10M solution in water). The reaction mix was stirred at 50°C for 1.5 days. The reaction was then diluted with water and extracted with ethyl acetate. The aqueous layer was acidified to pH<2 and was extracted again with ethyl acetate. The combined organic layers were washed with brine, dried on sodium sulfate, and the solvent was removed by evaporation under reduced pressure. The residue was purified by flash chromatography (10-50% linear gradient of ethyl acetate/hexanes, 1% acetic acid). Contaminating 2,16-heptadecanedione eluted at 15-20% ethyl acetate, while compound **3** eluted at 23-30% ethyl acetate. Pure compound **3** was obtained as a white solid (2g, 25%).

^{1}H NMR (400MHz, $CDCl_3$) δ 2.14 (t, *J* = 7.3, 2 H), 2.35 (t, *J* = 7.3, 2 H), 2.13 (s, 3 H), 1.63 (quint, *J* = 7.2, 2 H), 1.56 (quint, *J* = 6.9, 2 H), 1.25 (comp, 18 H); ^{13}C NMR (100MHz, $CDCl_3$) δ 209.71, 178.67, 43.99, 33.94, 30.00, 29.69, 29.66, 29.60, 29.58, 29.53, 29.34, 29.32, 29.18, 29.13, 24.83, 24.02. HRMS (ESI-q-TOF) m/z: $[M-H]^-$ Calculated for $C_{16}H_{29}O_3$ 269.2122; Found 269.2118.

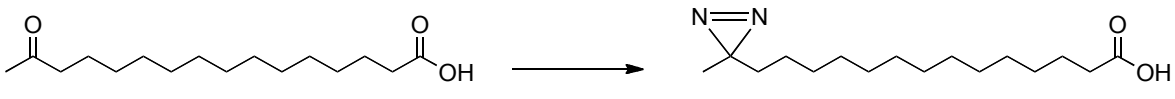

3 **4**

15-azi-hexadecanoic acid (4). Compound **3** (2g, 7.4mmol) was dissolved in dry methanol (15 mL), was cooled on ice, and ammonia gas was bubbled into the stirred solution. Within 10 minutes, a white precipitate formed. After 1 hour, hydroxylamine-O-sulfonic acid (1.67g, 14.8mmol, 2 equivalents) dissolved in dry methanol (5mL) was added. The reaction was stirred and ammonia bubbling was continued for another 2 hours, while allowing the reaction to warm to room temperature. After stopping ammonia bubbling, the reaction mix was diluted with methanol and was filtered to remove precipitated material. Triethylamine (2mL) was added to the filtrate, which was then concentrated *in vacuo*. The residue was dissolved in dry methanol (15mL) and triethylamine (4mL), after which iodine (10% in dry methanol) was added dropwise to the stirred solution, until the yellow color of iodine persisted. Stirring was continued for 3 hours at room temperature, after which sodium thiosulfate was added and the reaction was diluted with water. The solution was acidified (pH<2.0) and was extracted with ethyl acetate. The organic layers were washed with brine, dried on sodium sulfate, and concentrated *in vacuo*. The residue was purified by flash chromatography on silica gel (5-30% linear gradient of ethyl acetate/hexanes, 1% acetic acid). Compound **4** eluted at 5-10% ethyl acetate/hexanes, and was obtained as a white solid (580mg, 25%).

^{1}H NMR (400MHz, $CDCl_3$) δ 2.35 (t, *J* = 7.4, 2 H), 1.63 (quint, *J* = 7.5, 2 H), 1.33 (t, *J* = 7.8, 2 H), 1.24 (comp, 18 H), 1.16 (quint, *J* = 6.6, 2 H), 0.99 (s, 3 H); ^{13}C NMR (100MHz, $CDCl_3$) δ 180.22, 34.45, 34.20, 29.78, 29.72, 29.70, 29.61, 29.54, 29.37, 29.32, 29.28, 29.20, 26.05, 24.82, 24.16, 20.02. HRMS (ESI-q-TOF) m/z: $[M-H]^-$ Calculated for $C_{16}H_{29}N_2O_2$ 282.2307; Found 282.2311.

Fig. S1.

HPLC traces and mass spectrometric analysis of synthetic peptides used in this study.

Figure S1

ESI-MS Spectrum of palm-Shh22 peptide

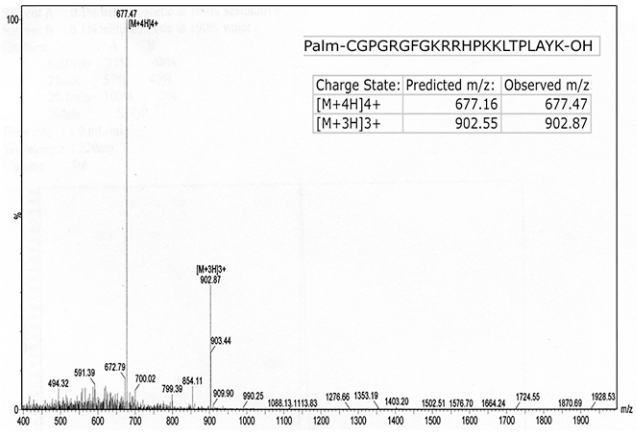

Chromatogram of palm-Shh22 peptide

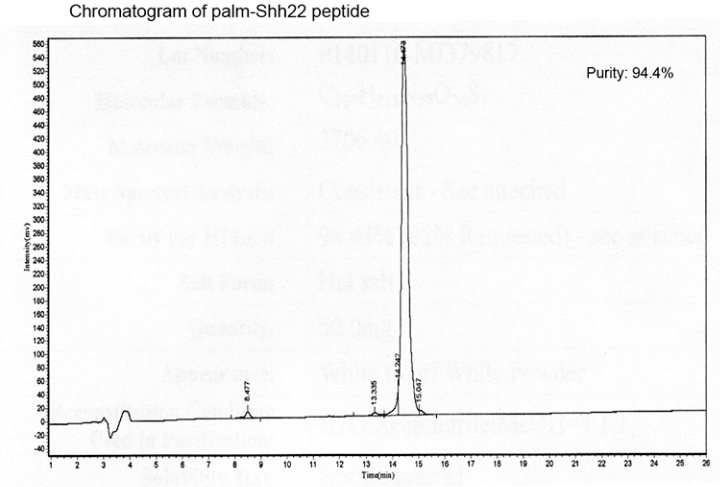

ESI-MS Spectrum of palm-Shh22C24S peptide

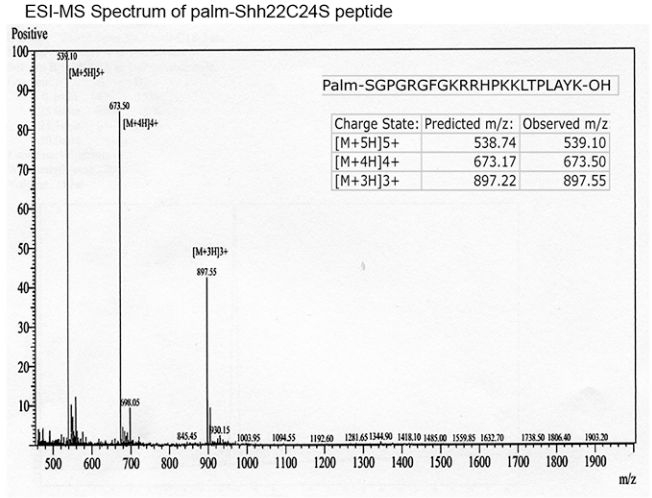

Chromatogram of palm-Shh22C24S peptide

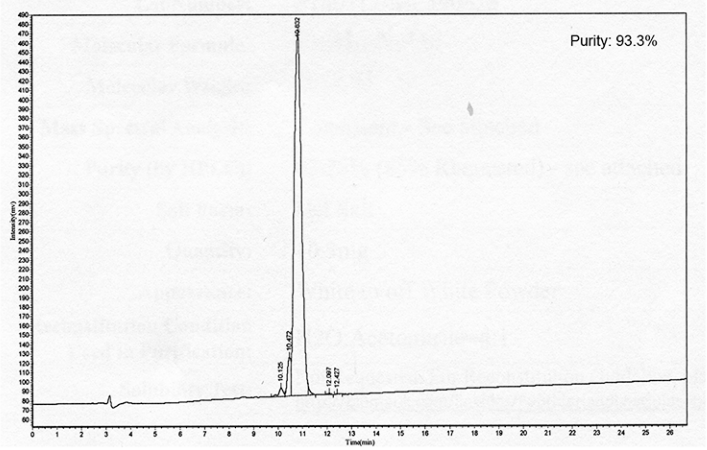

ESI-MS Spectrum of Shh22C24S peptide

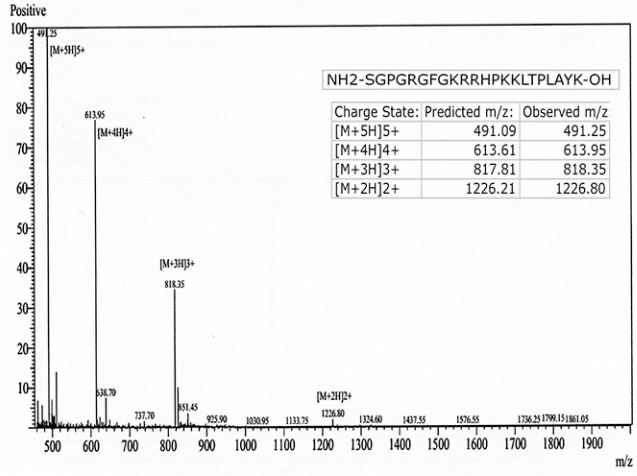

Chromatogram of Shh22C24S peptide

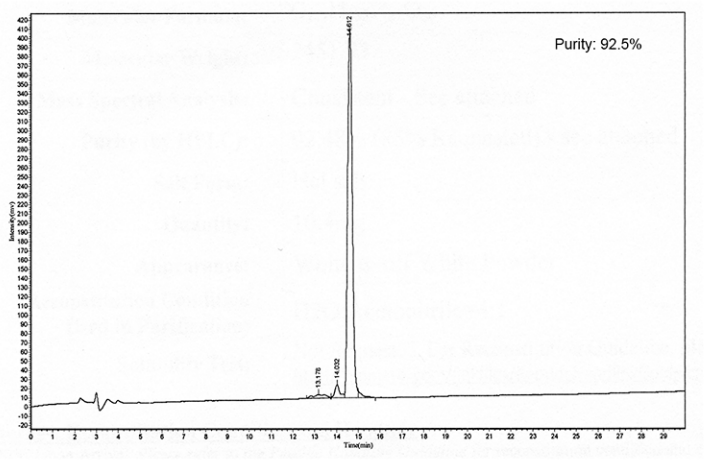

Figure S1 (continued)

ESI-MS Spectrum of palm-Shh9 peptide

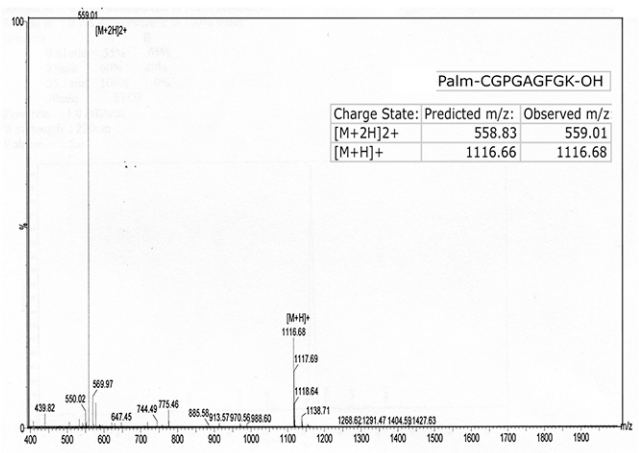

Chromatogram of palm-Shh9 peptide

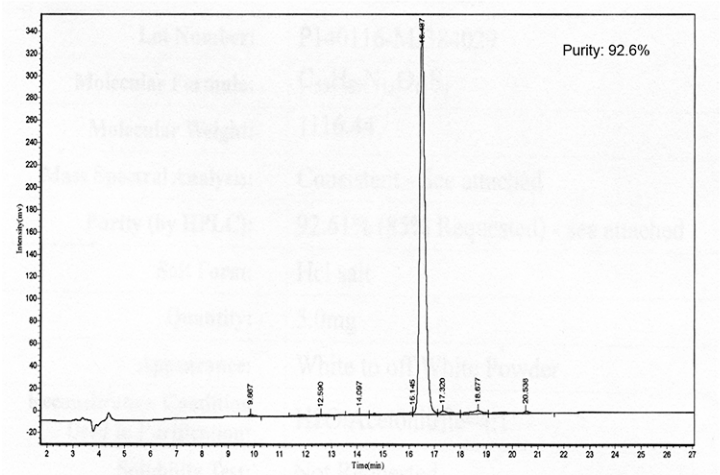

ESI-MS Spectrum of palm-Shh22P26A peptide

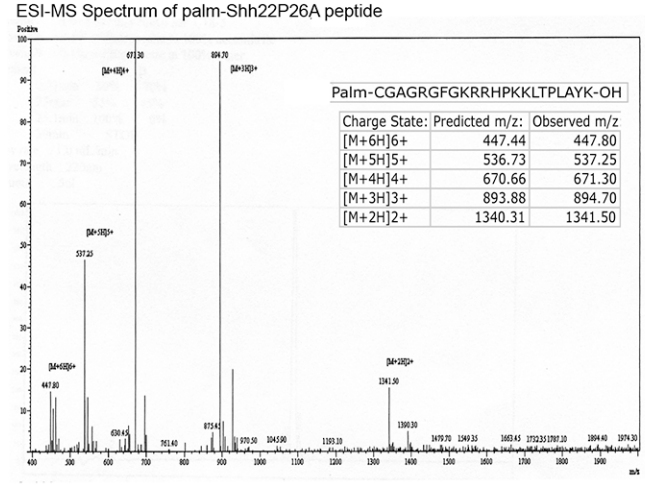

Chromatogram of palm-Shh22P26A peptide

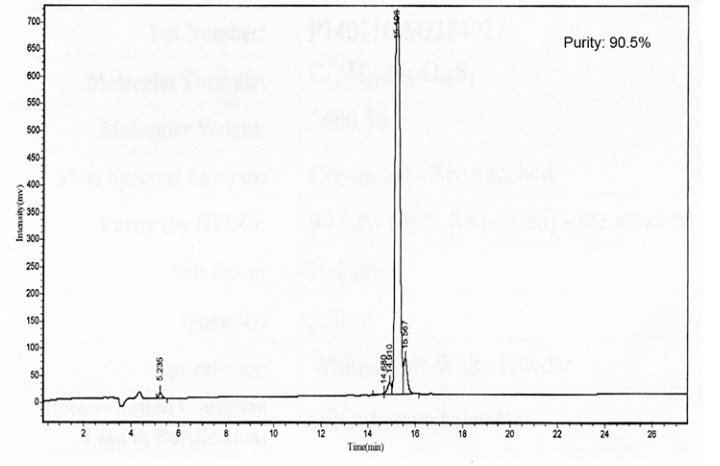

ESI-MS Spectrum of palm-Shh22R28A peptide

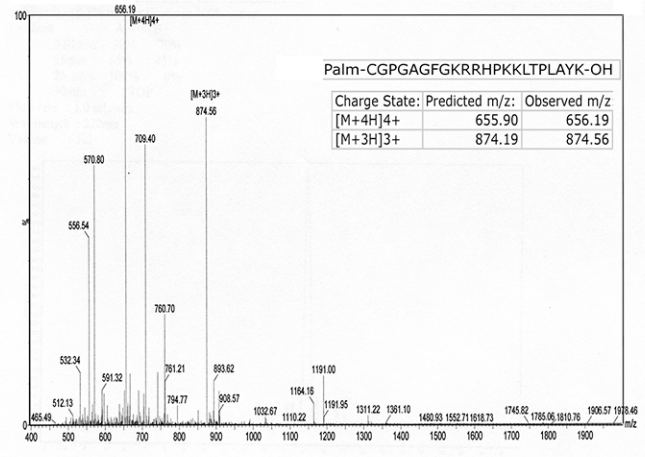

Chromatogram of palm-Shh22R28A peptide

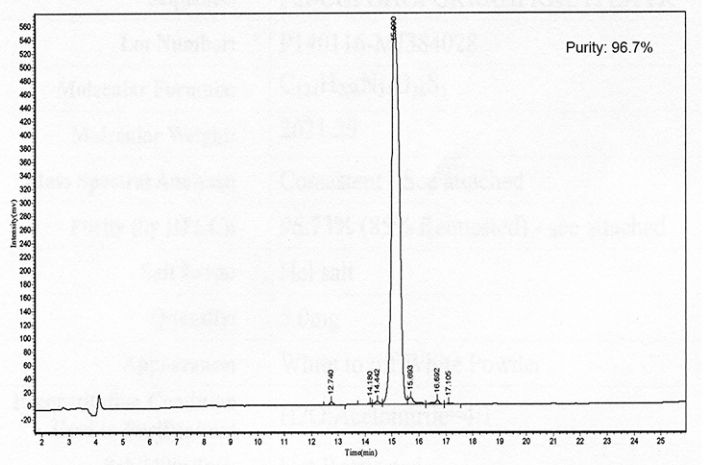

Figure S1 (continued)

ESI-MS Spectrum of Shh22-biotin peptide

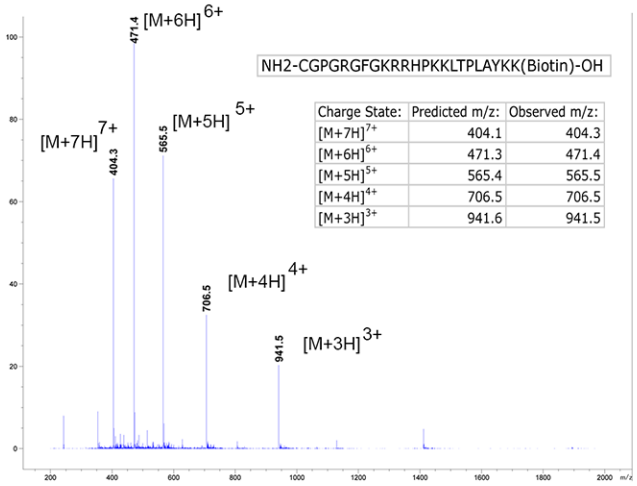

Charge State:	Predicted m/z:	Observed m/z:
$[M+7H]^{7+}$	404.1	404.3
$[M+6H]^{6+}$	471.3	471.4
$[M+5H]^{5+}$	565.4	565.5
$[M+4H]^{4+}$	706.5	706.5
$[M+3H]^{3+}$	941.6	941.5

Chromatogram of Shh22-biotin peptide

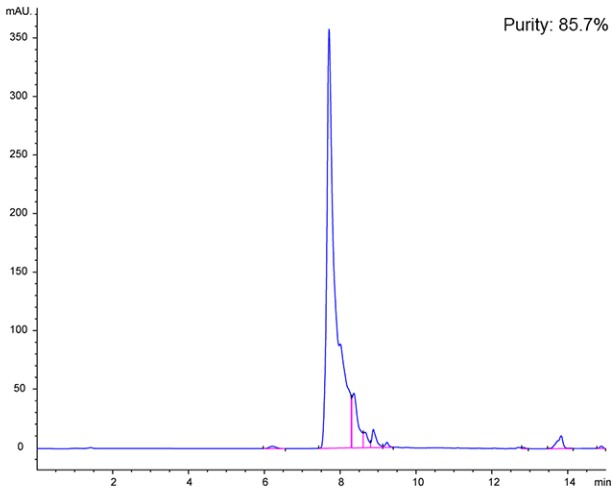

ESI-MS Spectrum of palm-Shh22-biotin peptide

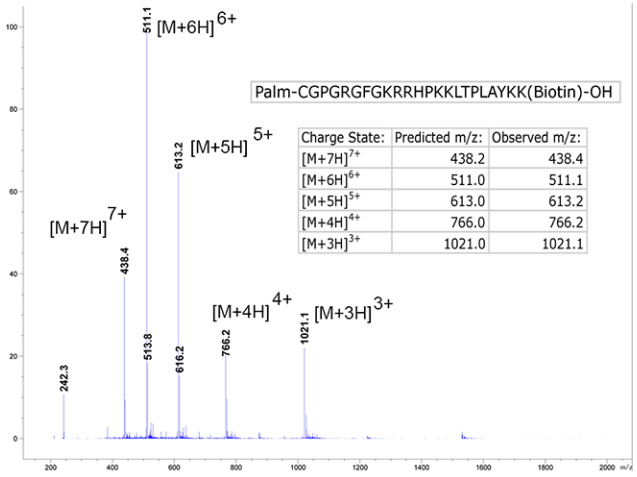

Charge State:	Predicted m/z:	Observed m/z:
$[M+7H]^{7+}$	438.2	438.4
$[M+6H]^{6+}$	511.0	511.1
$[M+5H]^{5+}$	613.0	613.2
$[M+4H]^{4+}$	766.0	766.2
$[M+3H]^{3+}$	1021.0	1021.1

Chromatogram of palm-Shh22-biotin peptide

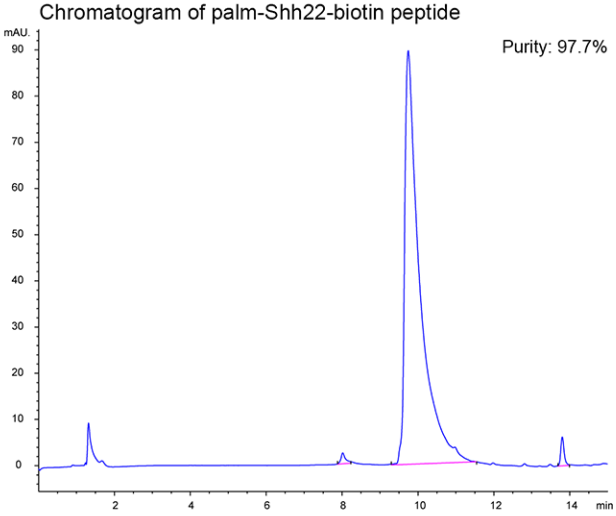

ESI-MS Spectrum of 15-azi-palm-Shh22-biotin peptide

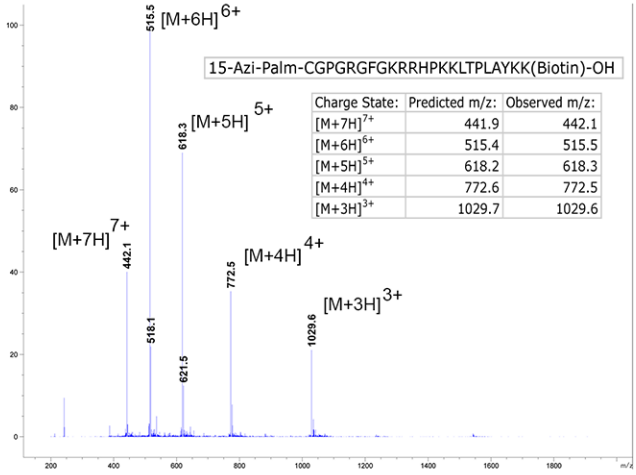

Charge State:	Predicted m/z:	Observed m/z:
$[M+7H]^{7+}$	441.9	442.1
$[M+6H]^{6+}$	515.4	515.5
$[M+5H]^{5+}$	618.2	618.3
$[M+4H]^{4+}$	772.6	772.5
$[M+3H]^{3+}$	1029.7	1029.6

Chromatogram of 15-azi-palm-Shh22-biotin peptide

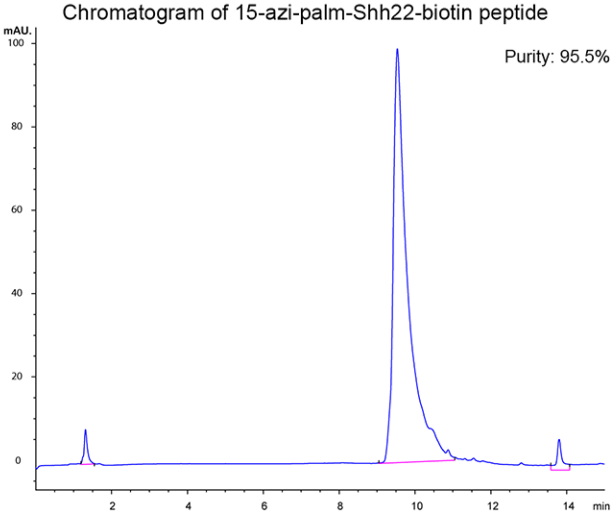

Fig. S2.

A palmitoylated Shh N-terminal fragment activates Hh signaling

(A) NIH-3T3 cells were incubated with control media, Shh22-HT, or Shh22-HT and SANT1 (1 μM). Endogenous Smo localization in cilia was measured by immunofluorescence and automated image analysis. The graph shows box plots of Smo fluorescence intensity in cilia, indicating the median and the 25th and 75th percentile of the distribution (n>300 cilia). Shh22-HT recruits endogenous Smo to cilia, which is reversed by SANT1.

(B) NIH-3T3 cells were incubated with control media, Shh, or Shh22-HT. Cell lysates were separated by SDS-PAGE, and were analyzed by immunoblotting with anti-Gli3 antibodies (to detect endogenous full-length Gli3 and the Gli3 repressor). Blotting for GSK3β was used as loading control. Both Shh22-HT and Shh cause Gli3R disappearance.

(C) As in (B), but cells were analyzed by immunoblotting with anti-Gli1 antibodies. Both Shh22-HT and Shh induce Gli1 protein accumulation, although Shh22-HT is weaker than Shh.

(D) The 5E1 antibody blocks signaling by Shh but not by palmitoylated Shh22 fragment. Shh Light II cells were incubated with control media, Shh, the palmitoylation site mutant ShhC24S, or Shh22-HT, in the presence or absence of 5E1 antibody, or of the Smo inhibitor, SANT1 (1 μM). Shh22-HT is not inhibited by 5E1, in contrast to Shh, while both Shh22-HT and Shh are inhibited by SANT1.

Figure S2

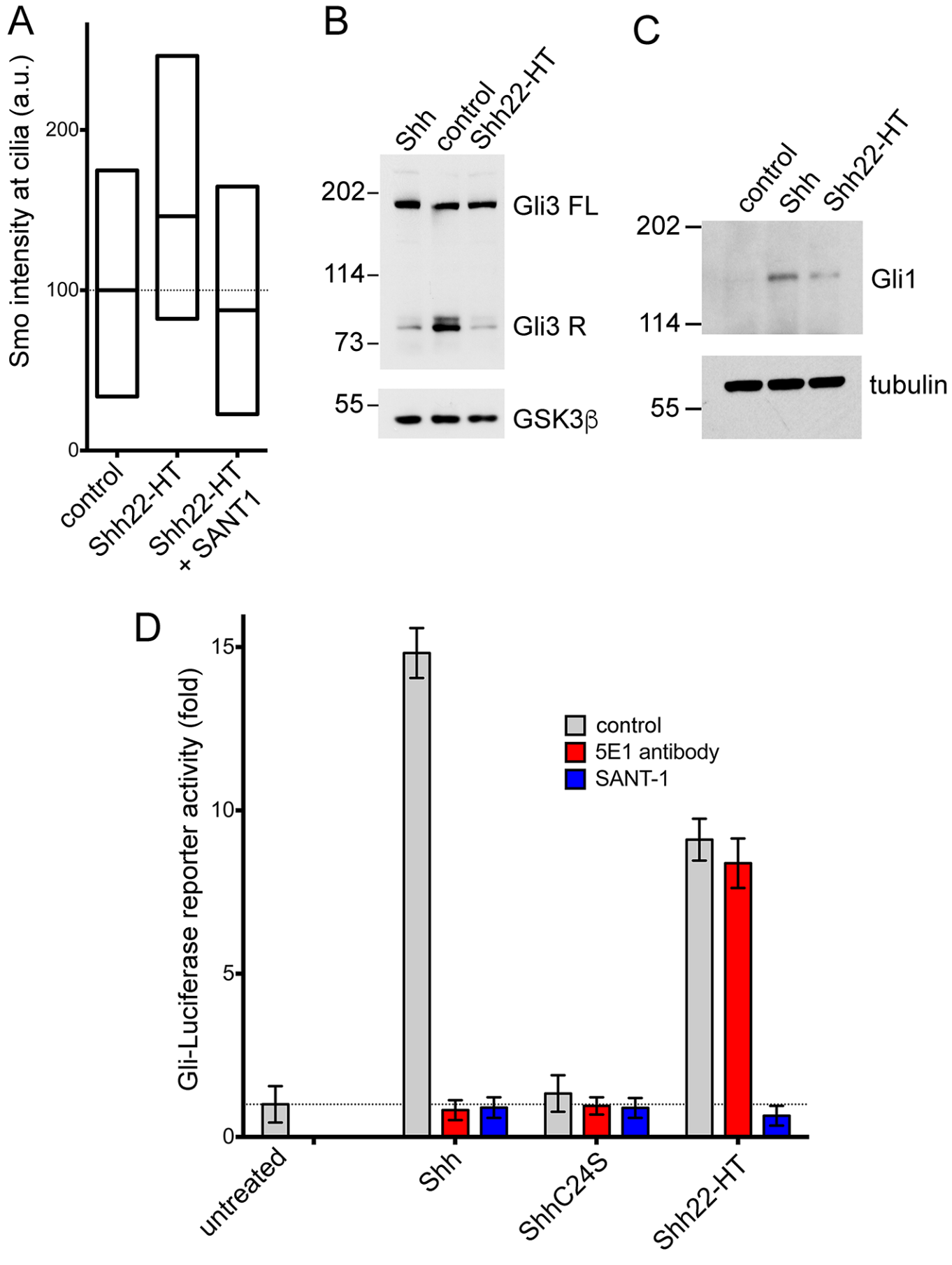
A
Smo intensity at cilia (a.u.)
200
100
0
control
Shh22-HT
Shh22-HT + SANT1
B
Shh
control
Shh22-HT
202
114
73
55
Gli3 FL
Gli3 R
GSK3β
C
control
Shh
Shh22-HT
202
114
55
Gli1
tubulin
D
Gli-Luciferase reporter activity (fold)
15
10
5
0
control
5E1 antibody
SANT-1
untreated
Shh
ShhC24S
Shh22-HT

Fig. S3.

Binding of palmitoylated N-terminal Shh peptide to Ptch1.

(A) Shh Light II cells were incubated with control media, Shh22-HT, Shh22-HT-TMR, Shh22C24S-HT, or Shh22C24S-HT-TMR. Hh pathway activity was measured by luciferase assay. Error bars represent standard deviation (n=3). TMR labeling does not affect Hh pathway activation by Shh22-HT.

(B) As in (A), but cells were treated with various concentrations of the synthetic peptides, 15-azi-palm-Shh22-biotin, palm-Shh22-biotin, or Shh22-biotin. The photoreactive peptide, 15-azi-palm-Shh22-biotin, activates Hh signaling, similar to palm-Shh22-biotin. Activation depends on 15-azi-palmitoylation, as the unmodified peptide, Shh22-biotin, is inactive.

(C) NIH-3T3 cells, stably expressing HA-tagged Ptch1, were incubated with 15-azi-palm-Shh22-biotin (3.5 μM), in the absence or presence of unlabeled competitor peptide, palm-Shh22 (10 μM). The cells were washed, UV-irradiated, and then lysed. Photocrosslinking was analyzed by affinity precipitation with streptavidin, followed by SDS-PAGE and immunoblotting with HA antibodies. The blot was stripped and subsequently probed with HRP-conjugated avidin. Arrowhead indicates full-length Ptch-HA.

Figure S3

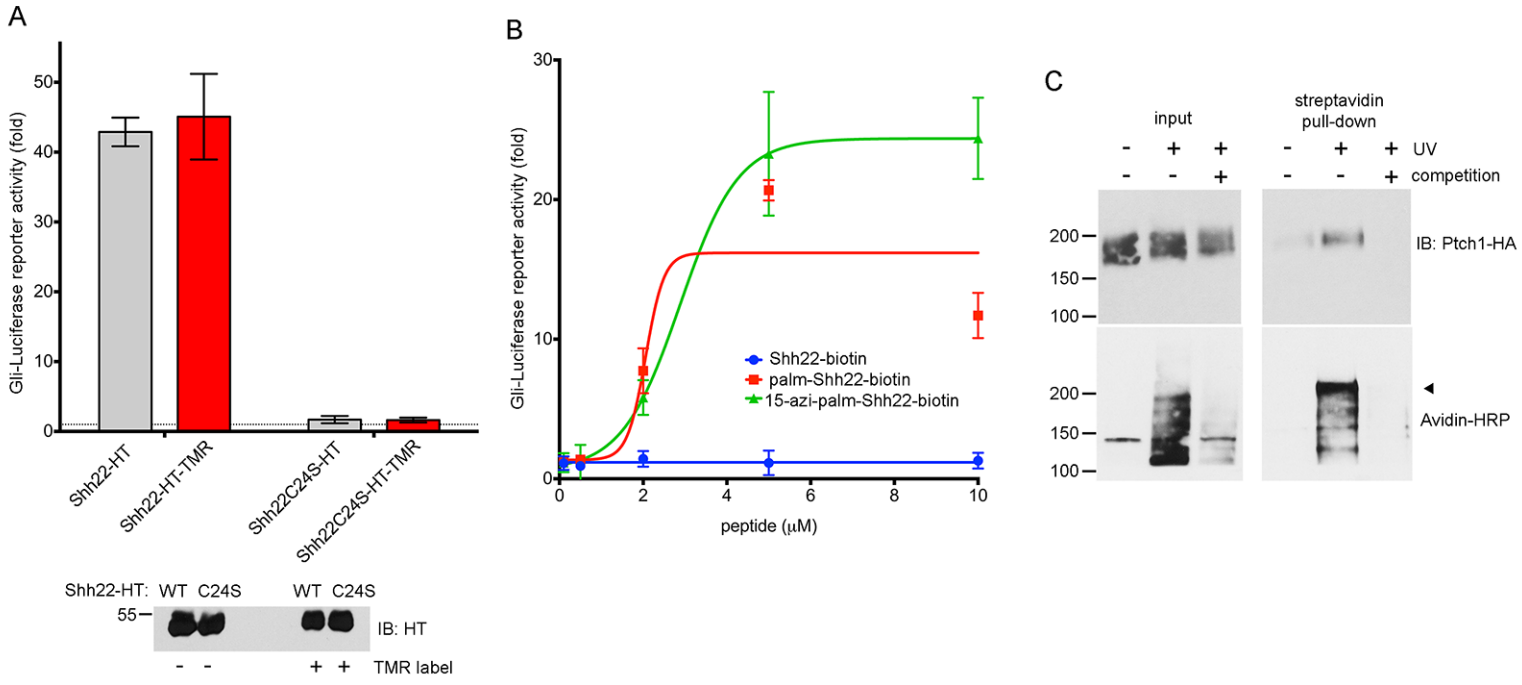
A
Gli-Luciferase reporter activity (fold)
Shh22-HT
Shh22-HT-TMR
Shh22C24S-HT
Shh22C24S-HT-TMR
Shh22-HT: WT C24S WT C24S
55
IB: HT
- - + + TMR label
B
Gli-Luciferase reporter activity (fold)
peptide (μM)
Shh22-biotin
palm-Shh22-biotin
15-azi-palm-Shh22-biotin
C
input
streptavidin pull-down
- + + - + + UV
- - + - - + competition
200
150
100
IB: Ptch1-HA
Avidin-HRP

Fig. S4.

Mouse Ptch1-null cells, stably expressing Ptch1Δloop2-eGFP or Ptch1-HA, were incubated with control media or Shh. Cell lysates were separated by SDS-PAGE and analyzed by immunoblotting for GFP, Gli1, Gli3R and GSK3β (loading control). The blot was then stripped and immunoblotted with HA antibodies. Both Ptch1Δloop2 and Ptch1 reverse constitutive Hh signaling, as shown by decreased Gli1 and increased Gli3R levels. Ptch1Δloop2 does not respond to Shh, in contrast to wild type Ptch1.

Figure S4

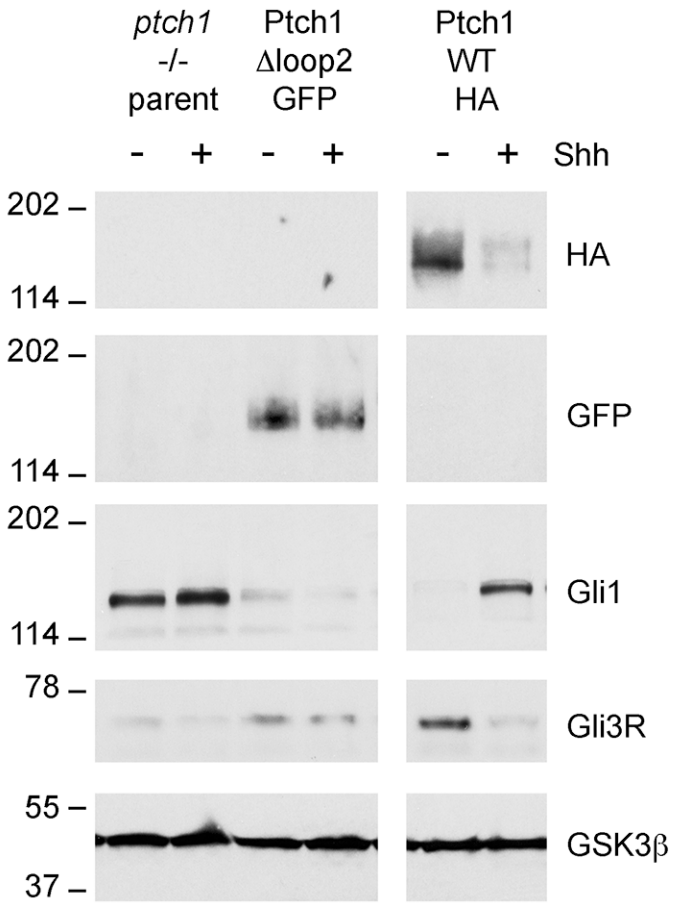
ptch1 -/- parent
Ptch1 Δloop2 GFP
Ptch1 WT HA
- + - + - + Shh
202
114
HA
202
114
GFP
202
114
Gli1
78
Gli3R
55
37
GSK3β

Fig. S5.

N-terminal cysteine is not necessary for activity of palm-Shh22 peptide.

Shh Light II cells were treated with various concentrations of the synthetic peptide palm-Shh22C24S, in which a serine residue replaces the N-terminal Cys24 residue, followed by measuring Hh pathway activity by luciferase assay. Error bars represent standard deviation (n=3 independent experiments). Palm-Shh22C24S activates Hh signaling in dose-dependent manner, suggesting that Cys24 is not absolutely required for activity, as long as a palmitoyl moiety is attached to the N-terminus. This experiment was performed in parallel with the experiment shown in Figure 1A, where data for the unpalmitoylated Shh22C24S peptide is shown. Note that palm-Shh22C24S appears more potent than palm-Shh22, which might be due to some degree of Cys24 oxidation in palm-Shh22.

Figure S5

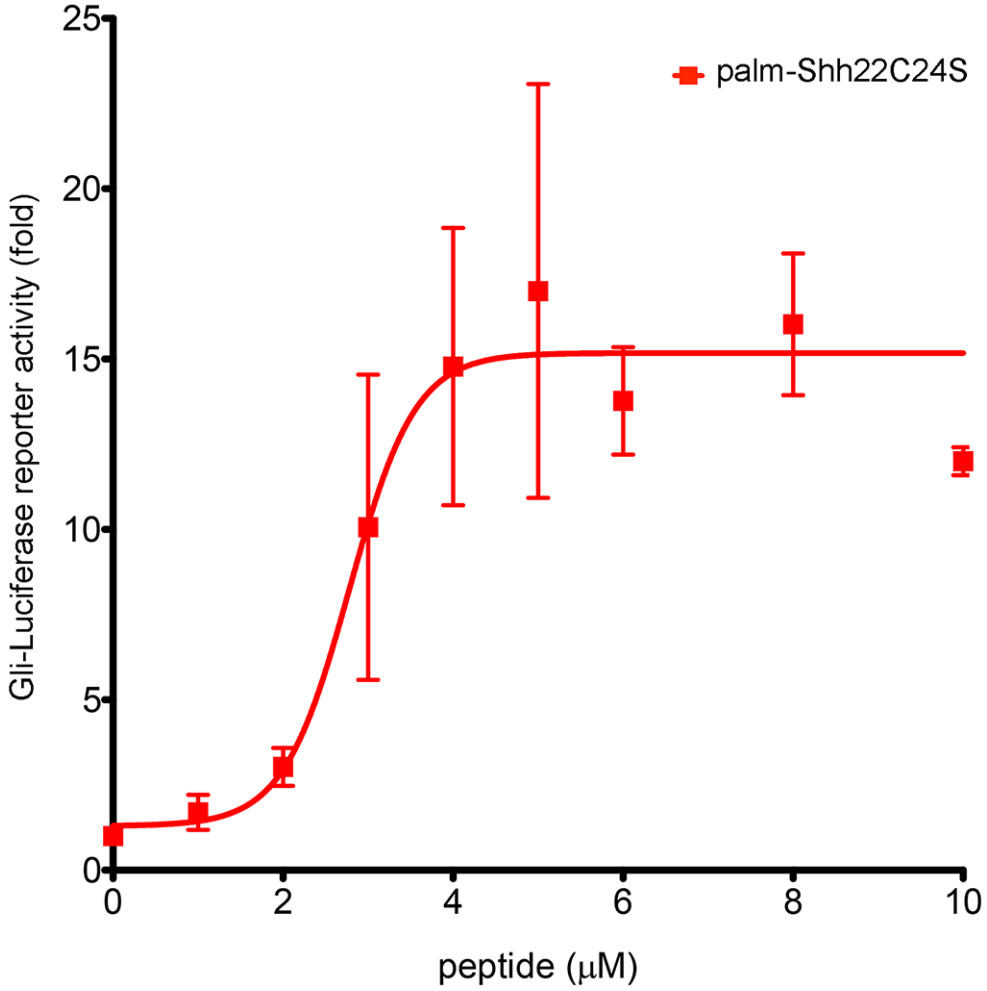
palm-Shh22C24S
Gli-Luciferase reporter activity (fold)
25
20
15
10
5
0
0
2
4
6
8
10
peptide (μM)

Fig. S6.

Palmitate and cholesterol modification of Shh are not required for Ptch1 internalization, but the palmitoylated N-fragment of Shh is essential for Ptch1 inhibition and signaling.

(A) Shh Light II cells were incubated with various concentrations of Shh, ShhC24S, or ShhΔ9, and Hh pathway activity was measured by luciferase assay. Error bars represent standard deviation (n=3). Equal volumes of the proteins were analyzed by SDS-PAGE and immunoblotting with anti-Shh antibodies (right panel). ShhΔ9 is inactive, while ShhC24S has much decreased activity relative to Shh.

(B) NIH-3T3 cells were incubated with control media, Shh, or ShhC24S. Transcription of the endogenous Hh target gene, Gli1, was measured by quantitative RT-PCR. Error bars represent standard deviation (n=3). Unpalmitoylated ShhC24S has much lower activity than Shh.

(C) NIH-3T3 cells, stably expressing Ptch1-eGFP, were incubated with control media, Shh, ShhC24S, cholesterol-modified Shh (ShhNp), or cholesterol-modified ShhC24S (ShhNpC24S). The two cholesterol-modified proteins were delivered in soluble form using Xenopus tropicalis Scube2 protein. The cells were processed for immunofluorescence, to detect Ptch1 and endogenous Smo, and the fraction of positive cilia was scored manually. Error bars represent standard deviation of the mean for three separate counts of n=30 cilia. All proteins cause Ptch1-eGFP internalization from cilia, but only Shh and ShhNp recruit endogenous Smo to cilia.

Figure S6

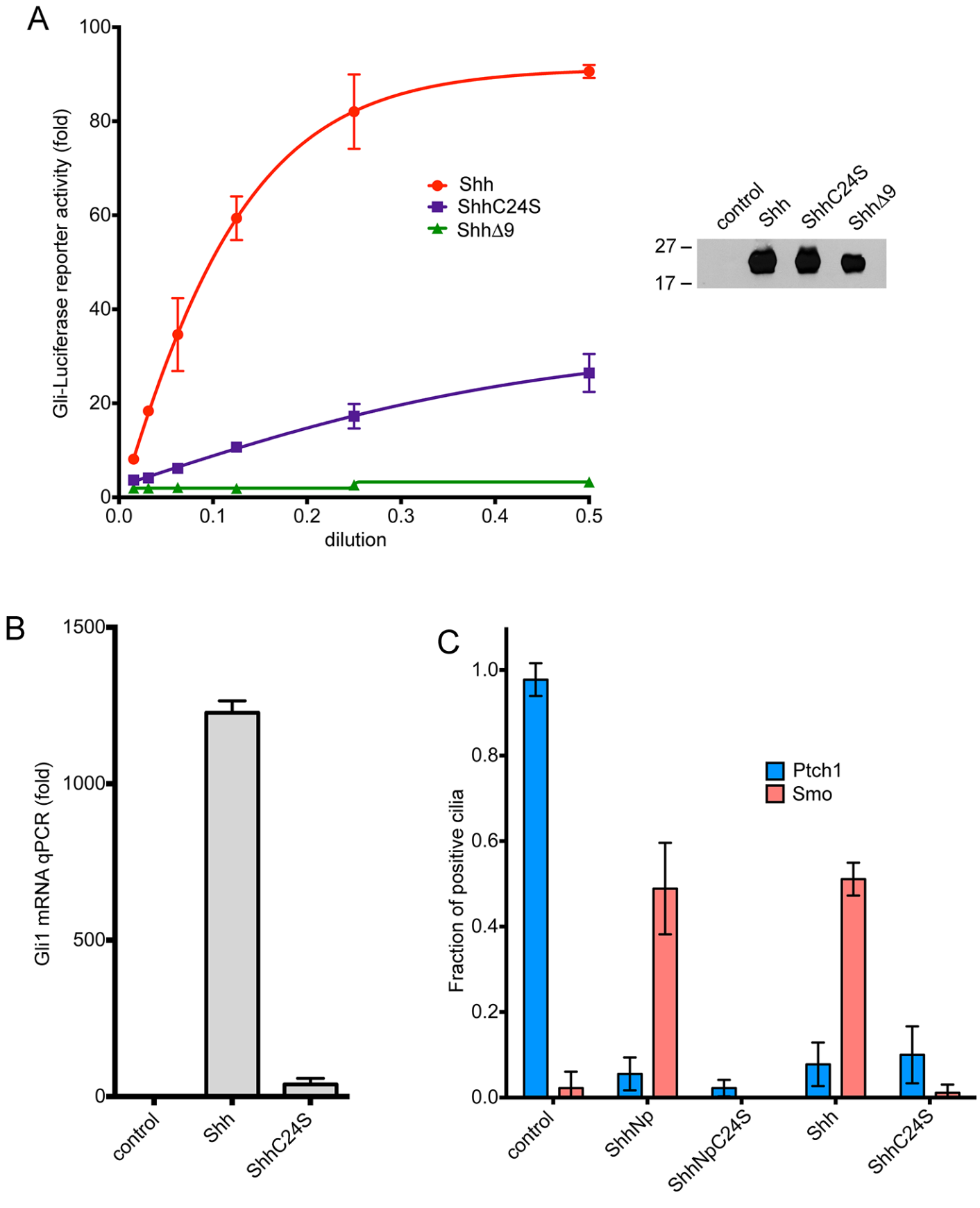
A
Gli-Luciferase reporter activity (fold)
dilution
Shh
ShhC24S
ShhΔ9
control
Shh
ShhC24S
ShhΔ9
27 –
17 –
B
Gli1 mRNA qPCR (fold)
control
Shh
ShhC24S
C
Fraction of positive cilia
Ptch1
Smo
control
ShhNp
ShhNpC24S
Shh
ShhC24S

Fig. S7.

Response of Gorlin Syndrome Ptch1 mutants to Shh.

(A) Ptch1-null cells, stably expressing the indicated eGFP-tagged Ptch1 constructs, were incubated with control media or Shh, and Ptch1 levels in cilia were measured by immunofluorescence and automated image analysis. Ciliary fluorescence is displayed as box plots, indicating the median intensity and the 25th and 75th percentile of the distribution (n>300 cilia). Ptch1G495V and Ptch1D499Y are removed from cilia in response to Shh, similar to wild type Ptch1.

(B) As in (A), but cells were treated with control media or SANT1 (1 μM), followed by measuring endogenous Smo localization at cilia. Ptch1G495V and Ptch1D499Y partially reverse Smo accumulation in cilia of Ptch1-null cells, consistent with their reduced activity compared to wild type Ptch1. In all cells, SANT1 abolishes Smo localization to cilia.

(C) Ptch1-null cells, stably expressing Ptch1-HA, Ptch1G495V-eGFP or Ptch1D499Y-eGFP, were incubated with control media or Shh. Cell lysates were analyzed by SDS-PAGE and immunoblotting for GFP, Gli1, Gli3R and GSK3β (loading control). The blot was then stripped and immunoblotted with HA antibodies. Ptch1G495V-eGFP and Ptch1D499Y-eGFP partially reverse constitutive Hh signaling, and respond to Shh.

Figure S7

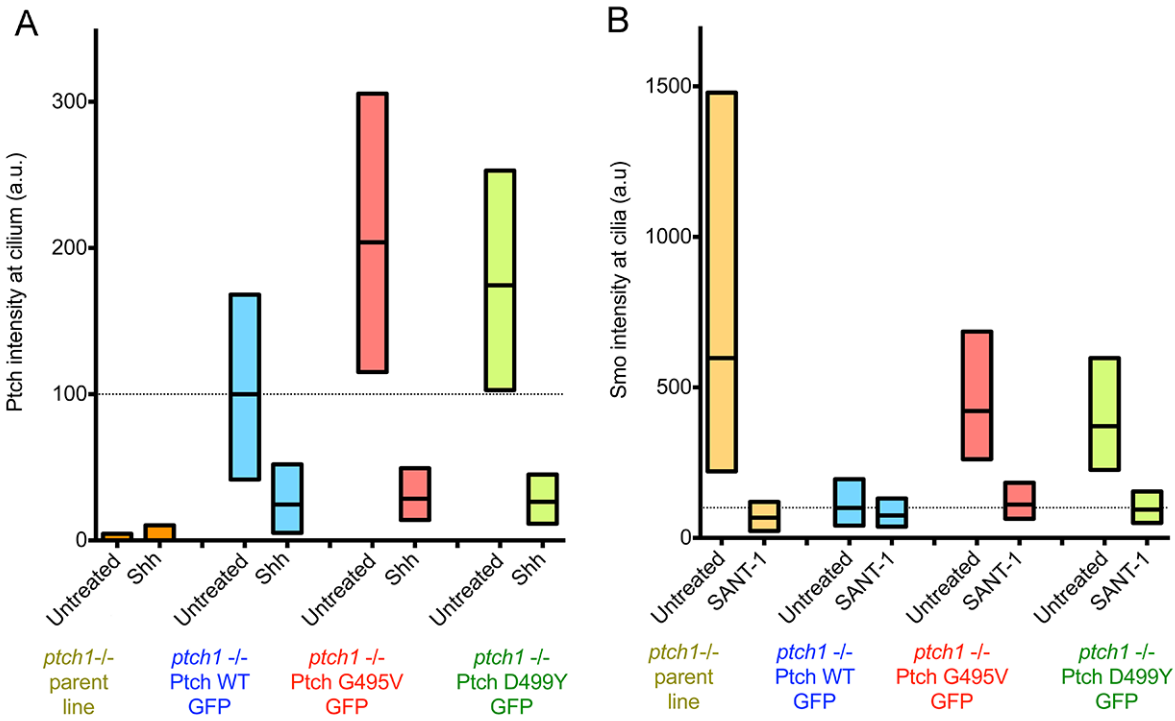
A
Ptch intensity at cilium (a.u.)
300
200
100
0
Untreated
Shh
ptch1-/- parent line
ptch1 -/- Ptch WT GFP
ptch1 -/- Ptch G495V GFP
ptch1 -/- Ptch D499Y GFP
B
Smo intensity at cilia (a.u)
1500
1000
500
0
Untreated
SANT-1

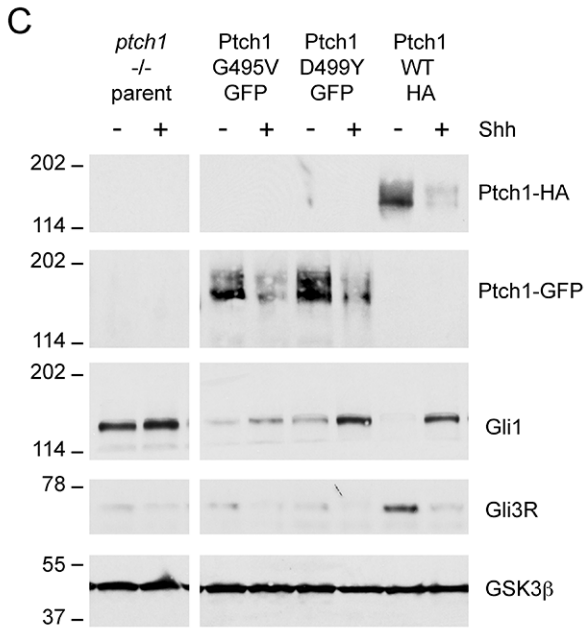
C
ptch1 -/- parent
Ptch1 G495V GFP
Ptch1 D499Y GFP
Ptch1 WT HA
- + - + - + - +
Shh
202 –
114 –
78 –
55 –
37 –
Ptch1-HA
Ptch1-GFP
Gli1
Gli3R
GSK3β